MATERIALS CHEMISTRY
FRONTIERS

Accepted Manuscript

This article can be cited before page numbers have been issued, to do this please use: R. W. Jadhav, R. V. Hangarge, M. D. Aljabri, K. S. More, J. Chen, L. A. Jones, R. A. Evans, J. Li, S. Bhosale and A. Gupta, *Mater. Chem. Front.*, 2020, DOI: 10.1039/D0QM00041H.

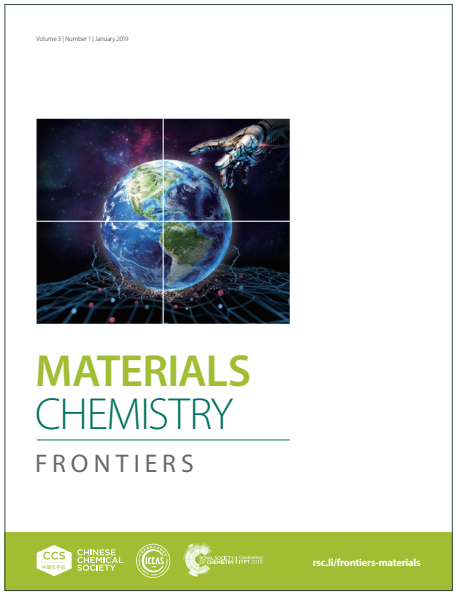

View Article Online
DOI: 10.1039/D0QM00041H

ARTICLE

# The first connection of carbonyl-bridged triarylamine and diketopyrrolopyrrole functionalities to generate a three-dimensional, non-fullerene electron acceptor

Received 00th January 20xx,
Accepted 00th January 20xx

DOI: 10.1039/x0xx00000x

Ratan W. Jadhav,[a,+] Rahul W. Hangarge,[a,b,1+] Mahmood D. Aljabri,[b,c,+] Kerba Shivaji More,[a] Jing-Yu Chen,[d] Lathe A. Jones,[b] Richard A. Evans,[e] Jing-Liang Li,*[d] Sheshanath V. Bhosale,*[a] Akhil Gupta*[e,f]

We report for the first time the use of a carbonyl-bridged triarylamine core with diketopyrrolopyrrole terminal units to generate a three-dimensional, non-planar non-fullerene electron acceptor with favourable properties for use in organic photovoltaic devices. The carbonyl-bridged triarylamine-functionalized, small molecule non-fullerene electron acceptor, 2,6,10-tris(5-(2,5-bis(2-ethylhexyl)-3,6-dioxo-4-(thiophen-2-yl)-2,3,5,6-tetrahydropyrrolo[3,4-*c*]pyrrol-1-yl)thiophen-2-yl)-4*H*-benzo[9,1]quinolizino[3,4,5,6,7-*defg*]acridine-4,8,12-trione (coded as **R1**), was synthesized *via* the industrially viable, Suzuki cross-coupling reaction using the commercially and cheaply available substrates. Using PTB7 as a donor, a power conversion efficiency of 9.33% was achieved in simple, solution-processable bulk-heterojunction devices, a result that is amongst the best in the literature for three-dimensional non-fullerene acceptors.

## 1. Introduction

Global population growth and economic development are generating ever-increasing demands on energy requirements, making the development of renewable energy technologies a pressing need. Natural resources such as sunlight, water and wind can supply renewable energy, with many approaches being developed to harvest solar energy at an affordable price. Organic and dye-sensitized solar cells are closer to becoming viable on the large scale due to extensive research efforts.[1,2] Organic or bulk-heterojunction (BHJ) devices in particular are a promising technology for lightweight, flexible, low-cost, remotely installed photovoltaic modules.[3] The active layer of such devices consists of donor and acceptor materials, in which fullerene derivatives such as [6,6]-phenyl-$C_{61}$-butyric acid methyl ester ($PC_{61}BM$), $PC_{71}BM$ and indene-$C_{60}$ bisadduct (ICBA) have dominated for more than two decades.[4] In terms of donor materials, conventional polymers such as poly-3-hexylthiophene (P3HT) have been studied in detail and have inspired the development of next-generation conjugated polymeric semiconductors such as PTB7 and PTB7-Th. Though power conversion efficiency (PCE) numbers of >10% can be achieved using the fullerene-based acceptors,[5] it seems that such acceptors have reached their limit and cannot reach higher performance using simple, scalable device fabrication strategies. This is due to several shortcomings such as limited absorption in the visible region, difficulty in synthesis and purification, morphological instability, and restricted chemical and energy level tuning *via* structural modification.[6] Furthermore, their high electron affinity can lead to a low open-circuit voltage.[7] Since these deficiencies restrain the performance of fullerene acceptors, researchers have been seeking alternative structural formats which can be easily generated, and can compete with fullerene acceptors by retaining appealing properties, such as strong accepting strength, solubility, and both chemical and thermal stabilities. These alternative molecules, otherwise termed non-fullerene acceptors, should meet other specifications such as adequate absorption from high to low energy regions, structural diversity and electronic tunability. Therefore, the design and development of a potential non-fullerene acceptor based on such necessities is a worthwhile challenge for both organic chemists and device physicists.

As such, there has been a dramatic surge in the development of non-fullerene acceptors (NFAs) indicating that a variety of structural types can be used as NFA targets.[8] The types such as acceptor-donor-acceptor, acceptor-acceptor-acceptor and three-dimensional with twisted configuration are the most successful and exploited structural types, with some examples possessing superior properties when compared to

[a] *School of Chemical Sciences, Goa University, Taleigao Plateau, Goa 403206, India; Email: svbhosale@unigoa.ac.in.*
[b] *Centre for Advanced Materials and Industrial Chemistry (CAMIC), School of Science, RMIT University, GPO Box 2476, Melbourne, Victoria 3001 Australia.*
[c] *Department of Chemistry, Al-Jumum University College, Umm Al-Qura University, Makkah 21955, Saudi Arabia.*
[d] *Institute for Frontier Materials, Deakin University, Waurn Ponds, Victoria 3216 Australia; Email: jingliang.li@deakin.edu.au*
[e] *CSIRO Manufacturing, Bayview Avenue, Clayton South, Victoria 3169 Australia.*
[f] *Department of Chemistry and Biotechnology, Faculty of Science, Engineering and Technology, Swinburne University of Technology, Hawthorn, Melbourne Victoria 3122 Australia. E-mail: akhilgk15@gmail.com; Tel: +61 402 131 118.*
+ Denotes equal contribution.
1 Present address: Tai Golwalkar Mahavidyalaya, Ramtek, District Nagpur, Maharashtra 441106, India.
Electronic Supplementary Information (ESI) available: [Fluorescence, theoretical absorption, PESA, CV, TGA, XRD curves, and experimental spectra]. See DOI: 10.1039/x0xx00000x

their fullerene-based counterparts.[9] The NFAs should be based on simple and scalable synthetic protocols, address the limitations of fullerene-based acceptors, and also have energy levels matching those of the conventional and conjugated polymeric and small molecular donor functionalities. However, many NFA targets based on these formats are small molecules that may exhibit higher crystallinity and large coplanar structures, resulting in excessive aggregation that leads to unfavourable blend surface morphologies. This issue can be solved with the development of non-planar or three-dimensional structural types, where strong intermolecular aggregation is minimised, whilst sustaining elongated and effective conjugation in each direction for photon harvesting. Furthermore, these formats can facilitate isotropic electron transport.[10] Therefore, it is reasoned that three-dimensional (3D) formats are a preferable choice to design efficient NFAs that favour superior blend morphology, resulting in high-performance devices.

One of the most effective strategies for designing non-planar, 3D acceptors is to construct a distorted structure with a central core, containing several electron-withdrawing end groups radiating from it. This central core can be conjugated or unconjugated depending upon the type of end group that is connected. The core determines the 3D conformation, contributes to intramolecular charge transfer (ICT) transition, and provides a rigid backbone for extended conjugation. A number of recent papers report key examples of NFAs based on 3D formats where a variety of cores have been used.[11] Among such cores, tetraphenylmethane, tetraphenylsilane, 9,9'-bifluorenylidene, 9,9'-spirobi[fluorene], 4,4'-spirobi[cyclopenta[2,1-b;3,4-b']dithiophene, truxene, spiro[fluorene-9,9'-xanthene] and tetraphenylethylene are the cores which have been exploited the most, but there is still a large scope for those structural units which can be centrally employed to generate non-planar, 3D targets.[8a,10]

To expand the structural diversity of NFAs, and to overcome the synthetic complexity of many materials reported previously, we have focussed our attention on a promising alternative building block; the carbonyl-bridged triarylamine (otherwise termed heterotriangulenes),[12] with three electron-withdrawing carbonyl groups. The carbonyl-bridged triarylamine (CBT) moiety acts as a moderate electron acceptor with appealing optoelectronic properties for organic electronic applications.[13] This unit has been reported as a building block for organic semiconductors with applications such as organic light emitting diodes, organic field-effect transistors,[14] and dye-sensitized solar cells,[15] and as electroluminescent materials.[16] Surprisingly, among the reported literature, no derivatives have been described that can be used as NFAs. Additional motivations for our interest in the design of a novel, 3D target based on CBT core were (1) the recent success that we were able to achieve using diketopyrrolopyrrole (DPP) as a terminal accepting group,[17] and (2) an understanding of the NFA research area that allows the control and prediction of the properties of a thoughtfully designed chromophore.[18] Taking into account the advantages exhibited by DPP unit, including strong accepting strength, low-cost synthesis and capability to be placed at terminal positions in a molecular structure, together with the literature precedence, herein we report the first combination of CBT and DPP functionalities to generate a non-planar, 3D small molecule NFA, 2,6,10-tris(5-(2,5-bis(2-ethylhexyl)-3,6-dioxo-4-(thiophen-2-yl)-2,3,5,6-tetrahydropyrrolo[3,4-*c*]pyrrol-1-yl)thiophen-2-yl)-4*H*-benzo[9,1]quinolizino[3,4,5,6,7-*defg*]acridine-4,8,12-trione [coded as **R1**], shown in Scheme 1.

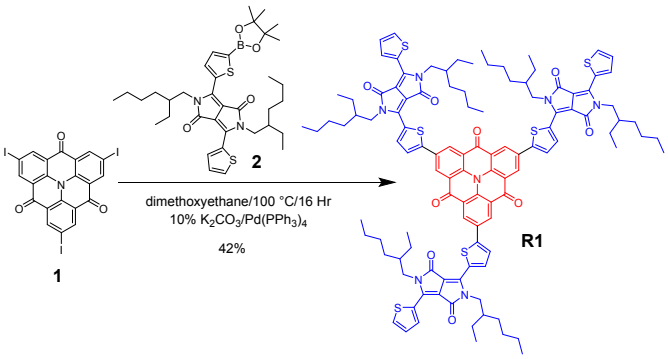


**Scheme 1**. Molecular structure of the newly designed non-fullerene acceptor (NFA) **R1** and its synthetic protocol.

## 2. Results and discussion

Compound **R1** was synthesized in a straightforward manner with moderate yield *via* the Suzuki cross-coupling reaction between 2,6,10-triiodo-4*H*-benzo[9,1]quinolizino[3,4,5,6,7-*defg*]acridine-4,8,12-trione (**1**) and the commercially available 2,5-bis(2-ethylhexyl)-3-(5-(4,4,5,5-tetramethyl-1,3,2-dioxaborolan-2-yl)thiophen-2-yl)-6-(thiophen-2-yl)-2,5-dihydropyrrolo[3,4-*c*]pyrrole-1,4-dione (**2**); see Scheme 1. The reaction was conducted in dimethoxyethane at 100 °C for 16 h using potassium carbonate ($K_2CO_3$; 10% aqueous solution) as a base and tetrakis(triphenylphosphine)palladium(0) [$Pd(PPh_3)_4$] as the catalyst. **R1** was purified through simple column chromatography and its structure was confirmed *via* proton spectroscopy, matrix-assisted laser desorption-ionization/time-of-flight (MALDI-TOF) measurement, and high-resolution mass spectrometry (HRMS) (for experimental spectra, see Electronic Supplementary Information (ESI†)). **R1** was found to be reasonably soluble in a variety of commonly used solvents, such as chloroform and dichlorobenzene, thus, fulfilling one of the major requirements of solution-processable organic electronics.

The optical and electrochemical properties of **R1** were characterized by ultraviolet-visible (UV-Vis) absorption spectroscopy and photoelectron spectroscopy in air. In solution, **R1** exhibited a strong absorption maximum ($\lambda_{max}$) at 590 nm (molar extinction coefficient ~ 80,000 L $M^{-1}$ $cm^{-1}$ at 5.50 μM). The absorption spectrum in solution displays a similar but slightly blue-shifted and narrower profile compared with that obtained in the film (pristine film $\lambda_{max}$ = 598 nm) (Fig. 1). The comparable absorption profiles in solution and film suggest that the non-planar, 3D structure of **R1** inhibits cofacial stacking of DPP units, enabling better charge separation and isotropic electron transport compared with fullerene derivatives.[19] The blend absorption profile of **R1** with two different donor

polymers, P3HT and PTB7, resulted in desirable broad absorption spectra, with the latter covering most of the visible spectrum (380–800 nm) when compared with the former (Fig. 1). The weak absorption of **R1** in the range of 650 nm to 800 nm compliments the absorption of PTB7, and is attributed to ICT between the central CBT core and terminal DPP units. This charge transfer is believed to favour high electron mobility. Furthermore, the blend films of **R1** displayed an ability to quench the fluorescence of neat films of **R1** (Fig. S1, ESI†), a result that provides valuable insight about the ability of donor-acceptor interface to dissociate excitons. This further confirms the potential of a material as an acceptor for organic photovoltaic devices.[20]

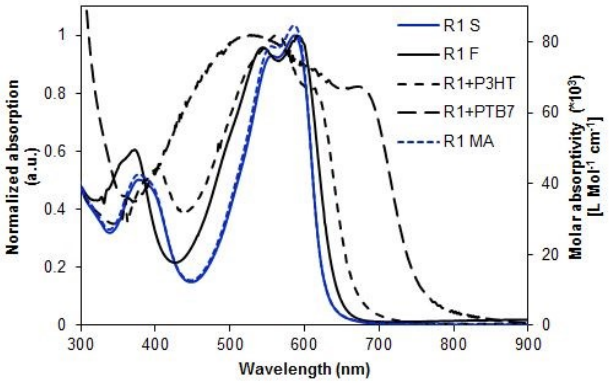


**Fig. 1.** The UV-Vis absorption spectra of **R1** (1) in chloroform solution (**R1** S), (2) as a pristine film (**R1** F), and (3) as a blend with P3HT (**R1** + P3HT) and PTB7 (**R1** + PTB7) [blend ratio = 1: 1.2 D: A (*w*/*w*)]. The molar absorptivity is represented by a dotted blue curve (**R1** MA; secondary Y-axis).

To obtain information about the theoretical density distribution of **R1**, time dependant-density functional theory (TD-DFT) calculations using the Gaussian 16 suite of programs and the B3LYP/6-311+G(d,p)//B3LYP/6-31G level of theory were carried out.[21] The calculations indicated that the gap between the highest occupied molecular orbital (HOMO) and the lowest unoccupied molecular orbital (LUMO) orbital densities is 2.15 eV. This value shows well segregated bands and guarantees an efficient charge transfer transition. The initial geometry optimization at the B3LYP/6-31G level of theory indicated a resemblance to the planar aromatic system which extended all the way to outer thiophene moieties. The HOMO density was symmetrically concentrated on the three peripheral thiophene moieties whereas the LUMO density was calculated to be a degenerate set of two orbitals concentrated on the CBT core of **R1** (see Fig. 2). The molecular electrostatic potential (MEP) map of **R1** as calculated using DFT at the B3LYP/6-311+G(d,p)//B3LYP/6-31G level of theory indicates a positive charge density on the central core, forming the acceptor part of the molecule, and a negative charge density on the peripheral thiophene moieties, forming the donor part of the molecule (see Fig. 2). Furthermore, the computed absorption spectrum shows a major transition peak at 662 nm, which is mainly described as the HOMO → LUMO transition (see Fig. S2, ESI†).

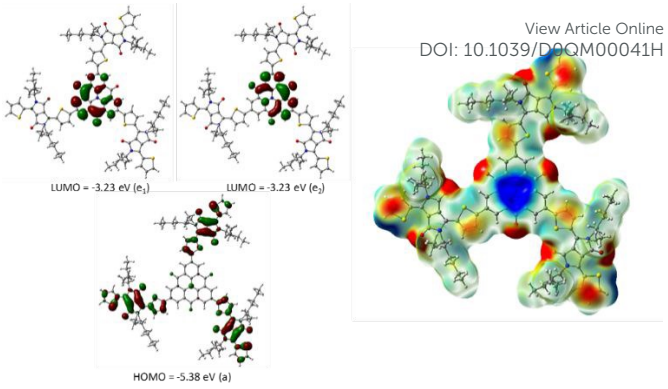


**Fig. 2.** Frontier molecular orbitals and orbital energies (left image), and molecular electrostatic potential (MEP) map (right image) of **R1** generated using TD-DFT at the B3LYP/6-311+G(d,p)//B3LYP/6-31G level of theory *in vacuo*.

The experimental estimation of the HOMO energy level was carried out using photoelectron spectroscopy in air (PESA), and the LUMO level was calculated by adding the optical band gap (film spectrum) to the HOMO value (for PESA spectrum, see Fig. S3, ESI†). The HOMO (-5.56 eV) and the LUMO (-3.74 eV) values are shown in the energy level diagram (see Fig. 3), which indicates that the energy levels of **R1** complements those of the commonly used donor polymers, P3HT and PTB7. The alignment of energy levels (Fig. 3) indicates that device incorporating such a combination of donor and acceptor semiconductors indeed guarantees a high open-circuit voltage ($V_{oc}$), which is clearly advantageous when compared with the device incorporating the conventional fullerene acceptor. Furthermore, cyclic voltammetry (CV) was conducted in dichloromethane, though **R1** was soluble in a variety of commonly used solvents such as chloroform, tetrahydrofuran and dichlorobenzene. The measurement of the HOMO energy levels using CV followed a similar trend as was established using PESA experiment (CV HOMO = 5.62 eV; PESA HOMO: = 5.56 eV). The cyclo-voltammogram indicated the presence of oxidation and reduction potentials, a result validating the existence of donor (peripheral thiophenes) and acceptor (CBT core) parts (Fig. S4, ESI for cyclic voltammograms) and of sufficient ICT. It is important to mention that although we observed the pristine and P3HT blend film spectra of **R1** somewhat similar, we still included P3HT for a fair comparison to see the performance of **R1** with the most-studied, benchmark donor polymer. We further realised that not only should organic semiconductors be soluble and chemically stable, they should also be thermally stable to allow device processing at higher temperatures. The thermal stability of **R1** was observed using thermogravimetric analysis. The thermogravimetric analysis (TGA) revealed that **R1** is a thermally stable chromophore and the organic solar cell device incorporating **R1** can be annealed, if required. For TGA spectrum, see Fig. S5, ESI†.

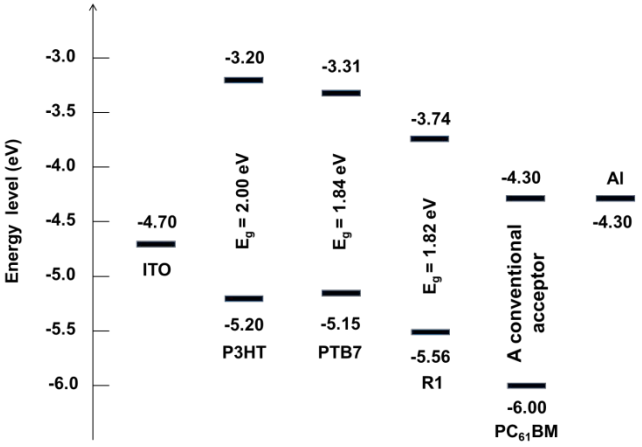


**Fig. 3.** Energy level diagram showing the alignment of different components of a BHJ device architecture based on **R1**.

Once it was established that **R1** displayed appropriate optical and electrochemical properties, we evaluated its performance as a NFA using two different, commercially available donor polymers, P3HT and PTB7, in solution-processable BHJ devices under simulated sunlight and monochromatic light illumination. The decision to test **R1** with the former and the historical benchmark polymer was primarily taken to understand its exciton dissociation efficacy. Having said that, we expected the outcome of P3HT-based devices to be inferior when compared with PTB7-based devices, given the latter's complementary absorption with **R1**. We chose a simple device architecture, indium-tin oxide (ITO)/poly(3,4-ethylenedioxythiophene):polystyrene sulfonate (PEDOT:PSS, 38 nm)/active layer (~75 nm)/Ca (20 nm)/Al (100 nm), where the active layer was a 1:1.2 blend of P3HT/PTB7: **R1**, respectively, spin-cast from *o*-dichlorobenzene atop the PEDOT:PSS surface. In context to the fabrication of fullerene-free organic solar cells, it is becoming evident that the use of a high boiling point solvent, such as *o*-dichlorobenzene, may affect device performance as it generally produces smoother blend films when compared with the films fabricated using low boiling point solvents such as chloroform. Taking advantage of this and our own understanding of the fabrication of fullerene-free materials, we annealed the active surfaces at 110 °C for five minutes. We also fabricated control devices based on the P3HT: $PC_{61}BM$ combination.

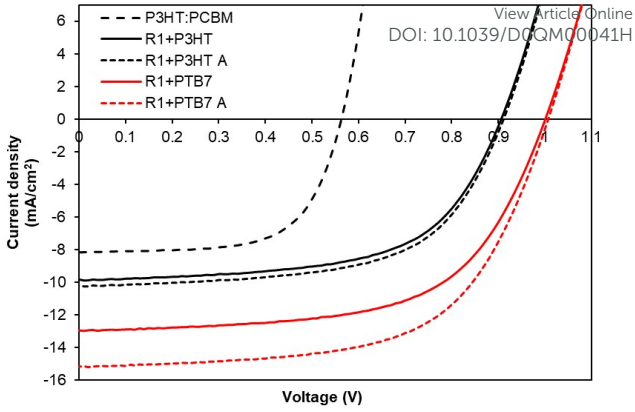


**Fig. 4.** Characteristic *J*–*V* curves for the best BHJ devices based on **R1** in blends with PTB7 and P3HT. Solid and square dotted lines correspond to pre-annealing and post-annealing (A) conditions, respectively, under simulated sunlight (100 mW $cm^{-2}$ AM 1.5G); blend ratio = 1: 1.2 *w*/*w* (D/A). The device structure was: ITO/PEDOT:PSS (38 nm)/active layer (~75 nm)/Ca (20 nm)/Al (100 nm).

With the PTB7: **R1** combination, the device parameters obtained were encouraging, i.e. $V_{oc}$, short-circuit current density ($J_{sc}$), fill factor (*FF*) and PCE reached 1.02 V, 15.20 mA $cm^{-2}$, 0.61 and 9.33%, respectively. With the P3HT: **R1** combination, the device parameters, $V_{oc}$, $J_{sc}$, *FF* and PCE, were 0.91 V, 10.20 mA $cm^{-2}$, 0.60, and 5.62%, respectively. The observance of high open-circuit voltages is consistent with the measured LUMO level of **R1** and the HOMO levels of the donor polymers. The unannealed devices with a similar donor: acceptor weight ratio provided a satisfactory outcome as well, and the observed PCE values were 7.89% and 5.32% with PTB7 and P3HT, respectively. In contrast, the maximum PCE reached 3.05% for a control device based on P3HT: $PC_{61}BM$, a result that corroborates most of the literature reports. For the current–voltage (*J*–*V*) curves and the detailed device parameters, see Fig. 4 and Table S1, ESI†, respectively.

The PTB7-based devices performed better than the devices based on P3HT under similar conditions. This improvement is mainly due to an increase in the $J_{sc}$, a finding that is consistent with the broader blend film spectrum of PTB7 and **R1**. A similar pattern was observed for the incident photon-to-current conversion efficiency (IPCE) measurement, where a much broader and stronger response was observed for PTB7-based devices when compared with the devices based on P3HT, see Fig. 5 for IPCE spectra. The IPCE maxima of 68% (at 591 nm) and 52% (at 580 nm) were achieved for PTB7- and P3HT-based devices, respectively. Though the broadness of these spectra indicated that both donor and acceptor components in active blends made a considerable contribution to the IPCE and $J_{sc}$, the PTB7-based spectrum spanned the whole visible region, ranging from 350 nm to 820 nm, suggesting better light-harvesting and a superior blending of donor and acceptor domains.

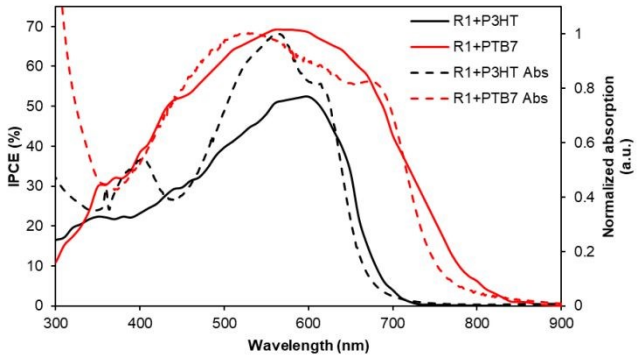


**Fig. 5.** The IPCE curves of the best performing devices described in Fig. 4. Solid lines correspond to the IPCE spectra whereas dotted lines represent blend film absorption profiles.

Furthermore, the photocurrents obtained from the IPCE data were in close agreement with those of the current–voltage measurements conducted under the one Sun conditions. The high-quality intermixing of donor and acceptor domains in case of PTB7 blend was confirmed using atomic force microscopy (AFM) analysis, which was conducted in tapping mode, where a much smoother surface was observed when compared with the P3HT blend. The actual surface morphologies of the blend films of P3HT: **R1** and PTB7: **R1** (1: 1.2 *w*/*w*) are shown in Fig. 6. The unannealed blend surfaces showed surface roughness of 2.88 nm (PTB7: **R1**) and 2.20 nm (P3HT: **R1**), suggesting that **R1** is a type of NFA that is evidently miscible with two different types of donor polymers, i.e. narrow and broad bandgap polymers. The annealed surfaces showed roughness of 3.16 nm (PTB7: **R1**) and 4.90 nm (P3HT: **R1**), a result that verifies the broad blend absorption due to effective intermixing of donor and acceptor domains. The surface roughness of P3HT blend grew larger upon annealing, a result that may be held responsible for the marginal improvement of device efficiency (5.62% *vs* 5.32%). Though it was evident through AFM analysis that the annealed blend morphology was superior to the as-cast blend, it was thought that annealing might have affected the morphology leading to a granular surface. The current literature implies that morphologies such as granular, bush and worm are generally preferred to morphologies such as amorphous, flat and regular, as the former morphologies tend to lead to better performing devices. Therefore, we conducted X-ray diffraction (XRD) analysis to probe surface crystallinity. It was found that both the blends were amorphous (see Fig. S6, ESI†), ruling out surface crystallinity and granular morphology upon annealing. Given the amorphous nature of the blends of **R1**, it can be argued that the target material's greater miscibility with the donor counterparts, and its strong light-harvesting ability together with complementary absorption with PTB7, play a key role for the observed performance. This further validates the premise of investigating NFAs based on 3D formats and underlines the utility of the functionalities used in designing **R1**.

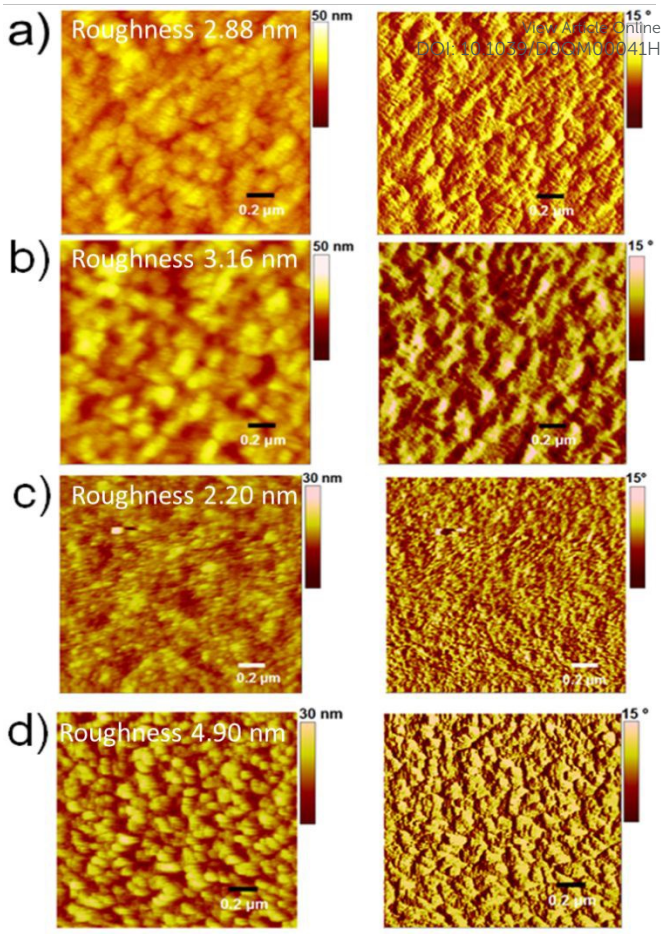


**Fig. 6.** AFM images for the unannealed and annealed blends of PTB7: **R1** (a and b, respectively) and P3HT: **R1** (c and d, respectively) with the specified weight ratios of 1: 1.2 (D: A). The root-mean square (RMS) roughness of 3.16 nm and 4.90 nm were observed for the annealed blend surfaces of PTB7 and P3HT, respectively.

## 3. Conclusions

In summary, a novel, carbonyl-bridged triarylamine-functionalized, 3D target material (coded as **R1**) was designed and synthesized, and its potential as a non-fullerene electron acceptor was demonstrated. The new material **R1** is structurally simple, adequately soluble, thermally stable, and highly absorbing in the visible region. These merits give **R1** the fundamental advantage over fullerene acceptors, such as $PC_{61}BM$, for which electronic and structural tuning, and limited absorption are restrictive factors. **R1** was designed to be non-planar, possessed energy levels complementing those of the routinely used and the commercially available donor polymers, P3HT and PTB7, and produced well-intermixed blend surfaces with these donors. The device parameters outlined herein are among the best numbers that have been achieved using the combination of a 3D NFA and the commercial donors. The results of this research evidently suggest that **R1** is an appropriately designed and highly promising acceptor that can be tested with a variety of donors, including polymers and small molecules, for future applications in BHJ devices.

## 4. Experimental details

### 4.1 Materials and methods

All the reactions were carried out under a nitrogen atmosphere, unless otherwise stated. Solvents used for various reactions were dried using a commercial solvent purification/drying system. Solvents used for extractions and column chromatography, and all other reagents were used as supplied by commercial vendors without further purifications or drying.

Thin layer chromatography (TLC) was performed using 0.25 mm thick plates pre-coated with Merck Kieselgel 60 $F_{254}$ silica gel, and visualized using UV light (254 and 365 nm). Petroleum spirits with a boiling point range of 40–60 °C were used wherever indicated. Column chromatography was performed on either 40–60 or 20–40 μm silica gel. $^1$H and $^{13}$C NMR spectra were recorded at 400 or 500 MHz, as indicated. The following abbreviations were used to explain multiplicities: s = singlet, d = doublet, t = triplet, q = quartet, m = multiplet, and dd = doublet of doublets. The chemical shifts were calibrated using residual non-deuterated solvent as an internal reference and are reported in parts per million ($\delta$) relative to tetramethylsilane ($\delta$ = 0). MALDI-TOF experiments were carried out using Autoflex III smart beam vertical mass spectrometer and for high resolution mass spectrometry, electrospray ionization (ESI) technique was used. PESA measurements were recorded using a Riken Keiki AC-2 PESA spectrometer with a power number of 0.5. Samples for PESA were prepared on ITO cleaned glass substrates and were run using a power setting of 10 nW. TGA experiments were carried out using a Q-500 TGA instrument with nitrogen as a purging gas. The samples were heated to 800 °C at a rate of 10 °C per minute under a nitrogen atmosphere. Electrochemical measurements were carried out using a PowerLab ML160 potentiostat interfaced via a PowerLab 4/20 controller to a PC running E-Chem For Windows version 1.5.2. The measurements were run in argon-purged dichloromethane with tetrabutylammonium hexafluorophosphate (0.1 M) as the supporting electrolyte. The cyclic voltammograms were recorded using a standard three electrode configuration with a glassy carbon (2mm diameter) working electrode, a platinum wire counter electrode and a silver wire pseudo reference electrode. The silver wire was cleaned in concentrated nitric acid followed by concentrated hydrochloric acid and then washed with deionised water. Cyclic-voltammograms were recorded with a sweep rate of 50 mV/sec. All the potentials were referred to the E-half of ferrocene/ferrocenium redox couple. Details of spectroscopic measurements, device fabrication and characterization of photovoltaic devices were reported previously.[17a] Atomic force microscopy topographic maps were directly performed on the active layers of PTB7: **R1** and P3HT: **R1** blends using an Asylum Research MFP-3D-SA instrument. The AFM was run in intermittent contact mode (tapping mode) using MicroMasch NSC18 tips (typical resonant frequency B100 kHz, typical probe radius B10 nm and typical aspect ratio 3: 1). A Bruker AXS D8 Discover instrument with a general area detector diffraction system (GADDS) using a CuKα source was utilized to obtain XRD patterns. Synthesis of 2,6,10-triiodo-4*H*-benzo[9,1]quinolizino[3,4,5,6,7-*defg*]acridine-4,8,12-trione was adapted from the published literature.[16]

**Synthesis of 2,6,10-tris(5-(2,5-bis(2-ethylhexyl)-3,6-dioxo-4-(thiophen-2-yl)-2,3,5,6-tetrahydropyrrolo[3,4-c]pyrrol-1-yl)thiophen-2-yl)-4H-benzo[9,1]quinolizino[3,4,5,6,7-defg]acridine-4,8,12-trione** (**R1**): In a 100 mL round bottom flask, $K_2CO_3$ (83 mg, 0.60 mmol) and $Pd(PPh_3)_4$ (14 mg, 0.012 mmol) were added to a solution of 2,6,10-triiodo-4*H*-benzo[9,1]quinolizino[3,4,5,6,7-*defg*]acridine-4,8,12-trione (**1**) (85 mg, 0.12 mmol) and 2,5-bis(2-ethylhexyl)-3-(5-(4,4,5,5-tetramethyl-1,3,2-dioxaborolan-2-yl)thiophen-2-yl)-6-(thiophen-2-yl)-2,5-dihydropyrrolo[3,4-*c*]pyrrole-1,4-dione (**2**) (395 mg, 0.60 mmol) in 1,2-dimethoxyethane (20 mL) under nitrogen atmosphere. The reaction mixture was stirred at 100 °C for 16 hrs. The progress of reaction was monitored through TLC. After completion, the reaction mixture was diluted with water and extracted with chloroform (2 × 30 mL). The combined organic layers were washed with water followed by brine and dried over anhydrous $MgSO_4$. The organic layer was filtered through Celite and concentrated under reduced pressure. The residue was purified by silica gel column chromatography eluting with 20 % ethyl acetate in hexanes to afford **R1** as a brick red powder (96 mg, 42%). $^1$H NMR (400 MHz, $CDCl_3$) $\delta$ 8.92 (d, $J$ = 3.9 Hz, 3H), 8.76 (s, 6 H), 8.48 (d, $J$ = 5.1 Hz, 3H), 7.48 (d, $J$ = 5.3 Hz, 3H), 7.44 (d, $J$ = 8.3 Hz, 3H), 7.11 (d, $J$ = 8.3 Hz, 3H), 3.97 (m, 12H), 1.82 (m, 6H), 1.45–1.15 (m, 48H), 0.93–0.82 (m, 36H); $^{13}$C NMR (400 MHz, $CDCl_3$) $\delta$ 173.8, 162.7, 142.3, 141.2, 141.0, 140.1, 139.8, 139.3, 138.9, 137.5, 137.3, 132.2, 130.6, 130.3, 130.0, 128.9, 128.8, 128.5, 124.1, 108.2, 45.9, 39.2, 36.6, 31.5, 30.3, 23.2, 14.1, 10.5; Autoflex III smart-beam vertical matrix-assisted laser desorption-ionization/time-of-flight (MALDI-TOF): without matrix: $[M]^+$ found for $C_{111}H_{123}N_7O_9S_6$ = 1889.770; with matrix trans-2-[3-(4-tert-Butylphenyl)-2-methyl-2-propenylidene]malononitrile (commonly known as DCTB): $[M]^+$ found for $C_{111}H_{123}N_7O_9S_6$ = 1889.740; HRMS **R1** (ESI): Calculated for $C_{111}H_{123}N_7O_9S_6$ = 1889.7741; found 1889.7701.

## Conflicts of interest

There are no conflicts to declare.

## Acknowledgements

M.D.A. is thankful to the Umm Al-Qura University (Saudi Arabia) for a full scholarship to study at RMIT University, Melbourne Australia. S.V.B. acknowledges the University Grant Commission (UGC) – Faculty Research Program (India) – for providing financial support and an award of professorship. CSIRO Manufacturing, Clayton, Victoria Australia is acknowledged for providing support through a Visiting Scientist position for A.G. M.D.A., J.Y.C. and A.G. acknowledge the vast variety of facilities at Swinburne, Deakin and RMIT Universities together with CSIRO Manufacturing, Clayton. A.G. acknowledges the assistance of Dr J. Subbiah at the University of Melbourne, Parkville, Melbourne, Victoria Australia.

## Notes and references


1 G. Yu, J. Gao, J. C. Hummelen, F. Wudl and A. J. Heeger, Polymer Photovoltaic Cells: Enhanced Efficiencies via a Network of Internal Donor-Acceptor Heterojunctions, *Science*, 1995, **270**, 1789–1791.

2 W. Xiang, A. Gupta, M. K. Kashif, N. Duffy, A. Bilic, R. A. Evans, L. Spiccia and U. Bach, Cyanomethylbenzoic Acid: An Acceptor for Donor-π-Acceptor Chromophores Used in Dye-sensitized Solar Cells, *ChemSusChem*, 2013, **6**, 256–260.

3 (*a*) G. Li, R. Zhu and Y. Yang, Polymer Solar Cells, *Nat. Photon.*, 2012, **6**, 153–161; (*b*) Y. Lin and X. Zhan, Oligomer Molecules for Efficient Organic Photovoltaics, *Acc. Chem. Res.*, 2016, **49**, 175–183; (*c*) L. Lu, T. Zheng, Q. Wu, A.M. Schneider, D. Zhao and L. Yu, Recent Advances in Bulk Heterojunction Polymer Solar Cells, *Chem. Rev.*, 2015, **115**, 12666–12731.

4 (*a*) F. Wudl, The Chemical Properties of Buckminsterfullerene (C60) and the Birth and Infancy of Fulleroids, *Acc. Chem. Res.*, 1992, **25**, 157–161; (*b*) C.-P. Chen, S.-H. Chan, T.-C. Chao, C. Ting and B.-T. Ko, Low-Bandgap Poly(Thiophene-Phenylene-Thiophene) Derivatives with Broaden Absorption Spectra for Use in High-Performance Bulk-Heterojunction Polymer Solar Cells, *J. Am. Chem. Soc.*, 2008, **130**, 12828–12833; (*c*) Y. He, H.-Y. Chen, J. Hou and Y. Li, Indene−$C_{60}$ Bisadduct: A New Acceptor for High-Performance Polymer Solar Cells, *J. Am. Chem. Soc.*, 2010, **132**, 1377–1382.

5 J. Zhao, Y. Li, G. Yang, K. Jiang, H. Lin, H. Ade, W. Ma and H. Yan, Efficient Organic Solar Cells Processed from Hydrocarbon Solvents, *Nat. Energy*, 2016, **1**, 15027.

6 R. Y. C. Shin, P. Sonar, P. S. Siew, Z. K. Chen and A. Sellinger, Electron-Accepting Conjugated Materials Based on 2-Vinyl-4,5-dicyanoimidazoles for Application in Organic Electronics, *J. Org. Chem*., 2009, **74**, 3293–3298.

7 (*a*) J. Zhao, Y. Li, H. Lin, Y. Liu, K. Jiang, C. Mu, T. Ma, J. Y. Lin Lai, H. Hu, D. Yu and H. Yan, High-efficiency Non-fullerene Organic Solar Cells Enabled by a Difluorobenzothiadiazole-based Donor Polymer Combined with a Properly Matched Small Molecule Acceptor, *Energy Environ. Sci*., 2015, **8**, 520–525; (*b*) C. Z. Li, H. L. Yip and A. K. Y. Jen, Functional Fullerenes for Organic Photovoltaics, *J. Mater. Chem*., 2012, **22**, 4161–4177.

8 (*a*) C. Yan, S. Barlow, Z. Wang, H. Yan, A. K. Y. Jen, S. R. Marder and X. Zhan, Non-fullerene Acceptors for Organic Solar Cells, *Nat. Rev. Mater.*, 2018, **3**, 18003; (*b*) N. Liang, W. Jiang, J. Hou and Z. Wang, New Developments in Non-fullerene Small Molecule Acceptors for Polymer Solar Cells, *Mater. Chem. Front.*, 2017, **1**, 1291–1303; (*c*) X. He, L. Yin and Y. Li, Design of Organic Small Molecules for Photovoltaic Application with High Open-circuit Voltage ($V_{oc}$), *J. Mater. Chem. C,* 2019, **7**, 2487–2521.

9 (*a*) D. Meng, D. Sun, C. Zhong, T. Liu, B. Fan, L. Huo, Y. Li, W. Jiang, H. Choi, T. Kim, J. Y. Kim, Y. Sun, Z. Wang and A. J. Heeger, High-Performance Solution-Processed Non-Fullerene Organic Solar Cells Based on Selenophene-Containing Perylene Bisimide Acceptor, *J. Am. Chem. Soc.,* 2016, **138**, 375–380; (*b*) Y. Lin, Q. He, F. Zhao, L. Huo, J. Mai, X. Lu, C. J. Su, T. Li, J. Wang, J. Zhu, Y. Sun, C. Wang and X. Zhan, A Facile Planar Fused-Ring Electron Acceptor for As-Cast Polymer Solar Cells with 8.71% Efficiency, *J. Am. Chem. Soc*., 2016, **138**, 2973–2976; (*c*) Y. Lin, F. Zhao, Q. He, L. Huo, Y. Wu, T. C. Parker, W. Ma, Y. Sun, C. Wang, D. Zhu, A. J. Heeger, S. R. Marder and X. Zhan, High-Performance Electron Acceptor with Thienyl Side Chains for Organic Photovoltaics, *J. Am. Chem. Soc.,* 2016, **138**, 4955–4961; (*d*) Y. J. Hwang, H. Li, B. A. E. Courtright, S. Subramaniyan and S. A. Jenekhe, Nonfullerene Polymer Solar Cells with 8.5% Efficiency Enabled by a New Highly Twisted Electron Acceptor Dimer, *Adv. Mater.*, 2016, **28**, 124–131; (*e*) A. Rananaware, A. Gupta, J. Li, A. Bilic, L. Jones, S. Bhargava and S. V. Bhosale, A Four-directional Non-fullerene Acceptor Based on Tetraphenylethylene and Diketopyrrolopyrrole Functionalities for Efficient Photovoltaic Devices with a High Open-circuit Voltage of 1.18 V, *Chem. Commun*., 2016, **52**, 8522–8525.

10 G. Zhang, J. Zhao, P. C. Y. Chow, K. jiang, J. Zhang, Z. Zhu, J. Zhang, F. Huang and H. Yan, Non-fullerene Acceptor Molecules for Bulk Heterojunction Organic Solar Cells, *Chem. Rev*., 2018, **118**. 3447–3507.

11 (*a*) R. Geng, *et al.*, Non-fullerene Acceptor for Organic Solar Cells with Chlorination on Dithieno[3,2-*b*:2′,3′-*d*]pyrrol Fused-Ring, *ACS Energy Lett.*, 2019, **4**, 763–770; (*b*) D. Srivani, *et al.*, Naphthalene Diimide-based Non-fullerene Acceptors Flanked by Open-ended and Aromatizable Acceptor Functionalities, *Chem. Commun*., 2017, **53**, 11157–11160; (*c*) W. Chen and Q. Zhang, Recent Progress in Non-fullerene Small Molecule Acceptors in Organic Solar Cells (OSCs), *J. Mater. Chem. C*, 2017, **5**, 1275–1302; (*d*) H. Sun, P. Sun, C. Zhang, Y. Yang, Z. Gao, F. Chen, Z. Xu, Z. K. Chen and W. Huang, High-Performance Organic Solar Cells Based on a Non-Fullerene Acceptor with a Spiro Core, *Chem. Asian. J*., 2017, **12**, 721–725; (*e*) N. Qiu, Z. Yang, H, Zhang, Z. Wan, C. Li, F, Lie, H. Zhang, T. P. Russell and Y. Chen, Non-fullerene Small Molecular Acceptors with a Three-Dimensional (3D) Structure for Organic Solar Cells, *Chem. Mater*., 2016, **28**, 6770–6778; (*f*) M. Chang, Y. Wang, N. Qiu, Y. Q. Q. Yi, Z. Wan, C. Li and Y. Chen, A Three-dimensional Non-fullerene Small Molecule Acceptor for Solution-processed Organic Solar Cells, *Chin. J. Chem*., 2017, **35**, 1687–1692.

12 (*a*) D. Hellwinkel and M. Melan, Heteropolycyclen vom Triangulen-Typ, I. 8.12-Dihydro-4H-benzo[1.9]chinolizino[3.4.5.6.7-*defg*]acridin-trion-(4.8.12) und 5.9-Dihydro-chino[3.2.1-*de*]acridin-dion-(5.9), *Chem. Ber.*, 1971, **104**, 1001–1016; (*b*) D. Hellwinkel and M. Melan, Heteropolycyclen vom Triangulen-Typ, II. Zur Stereochemie verbrückter Triarylamine, *Chem. Ber*., 1974, **107**, 616–626.

13 (*a*) S. Paek, N. Cho, S. Cho, J. K. Lee and J. Ko, Planar Star-Shaped Organic Semiconductor with Fused Triphenylamine Core for Solution-Processed Small-Molecule Organic Solar Cells and Field-Effect Transistors, *Org. Lett*., 2012, **14**, 6326–6329; (*b*) Z. Fang, V. Chellappan, R. D. Webster, L. Ke, T. Zhang, B. Liu, Y.-H. Lai and Y.-H. Lai, Bridged-triarylamine Starburst Oligomers as Hole Transporting Materials for Electroluminescent Devices, *J. Mater. Chem.*, 2012, **22**, 15397–15404.

14 (*a*) A. V. Gorbunov, A. T. Haedler, T. Putzeys, R. H. Zha, H.-W. Schmidt, M. Kivala, I. Urbanavičiūtė, M. Wübbenhorst, E. W. Meijer and M. Kemerink, Switchable Charge Injection Barrier in an Organic Supramolecular Semiconductor, *ACS. Appl. Mater. Interfaces*, 2016, **8**, 15535–15542; (*b*) C. Liu, Y. Li, Y. Zhang, C. Yang, H. Wu, J. Qin and Y. Cao, Solution-Processed, Undoped, Deep-Blue Organic Light-Emitting Diodes Based on Starburst Oligofluorenes with a Planar Triphenylamine Core, *Chem. Eur. J.*, 2012, **18**, 6928–6934.

15 K. Do, D. Kim, N. Cho, S. Peak, K. Song and J. Ko, New Type of Organic Sensitizers with a Planar Amine Unit for Efficient Dye-Sensitized Solar Cells, *Org. Lett.,* 2012, **14**, 222–225.

16 H. Zhang, S. Wang, Y. Li, B. Zhang, C. Du, X. Wan and Y. Chen, Synthesis, Characterization, and Electroluminescent Properties of Star Shaped Donor–Acceptor Dendrimers with Carbazole Dendrons as Peripheral Branches and Heterotriangulene as Central Core, *Tetrahedron*, 2009, **65**, 4455–4463.

17 (*a*) S. M. Wagalgave, *et al.*, An Efficient, Three-dimensional Non-fullerene Electron Acceptor: Functionalizing Tetraphenylethylene with Naphthalene diimides, *Mater. Chem. Front.*, 2019, **3**, 1231–1237; (*b*) H. Patil, W. X. Zu, A. Gupta, V. Chellappan, A. Bilic, P. Sonar, A. Rananaware, S. V. Bhosale and S. V. Bhosale, A Non-fullerene Electron Acceptor Based on Fluorene and Diketopyrrolopyrrole Building Blocks for Solution-processable

View Article Online
DOI: 10.1039/D0QM00041H

Organic Solar Cells with an Impressive Open-circuit Voltage, *Phys. Chem. Chem. Phys*., 2014, **16**, 23837–23842.

18 (*a*) A. Rananaware, A. Gupta, G. Kadam, D. D. La, A. Bilic, W. Xiang, R. A. Evans and S. V. Bhosale, Cyanopyridone Flanked the Tetraphenylethylene to Generate an Efficient, Three-dimensional Small Molecule Non-Fullerene Electron Acceptor, *Mater. Chem. Front*., 2017, **1**, 2511–2518; (*b*) G. Kadam, Anuradha, A. Agarwal, A. Puyad, D. D. La, R. A. Evans, J. Li, A. Gupta and S. V. Bhosale, Generating A Three-dimensional Non-Fullerene Electron Acceptor by Combining Inexpensive Spiro[fluorene-9,9'-xanthene] and Cyanopyridone Functionalities, *Mater. Chem. Front*., 2018, **2**, 1090–1096; (*c*) A. Gupta, A. Rananaware, P. S. Rao, D. D. La, A. Bilic, W. Xiang, J. Li, R. A. Evans, S. V. Bhosale and S. V. Bhosale, An H-shaped, Small Molecular Non-fullerene Acceptor for Efficient Organic Solar Cells with an Impressive Open-circuit Voltage of 1.17 V, *Mater. Chem. Front*., 2017, **1**, 1600–1606; (*d*) P. S. Rao, A. Gupta, D. Srivani, S. V Bhosale, A. Bilic, J. Li, W. Xiang, R. A. Evans and S. V. Bhosale, An Efficient Non-fullerene Acceptor Based on Central and Peripheral Naphthalene Diimides, *Chem. Commun*., 2018, **54**, 5062–5065; (*e*) D. Srivani, A. Gupta, S. V. Bhosale, A. L. Puyad, W. Xiang, R. A. Evans and S. V. Bhosale, Non-fullerene Acceptors Based on Central Naphthalene Diimide Flanked by Rhodanine or 1,3-Indanedione, *Chem. Commun*., 2017, **53**, 7080–7083.

19 S. Rajaram, R. Shivanna, S. K. Kandappa and K. S. Narayan, Nonplanar Perylene Diimides as Potential Alternatives to Fullerenes in Organic Solar Cells, *J. Phys. Chem. Lett*., 2012, **3**, 2405–2408.

20 A. M. Raynor, A. Gupta, H. Patil, A. Bilic and S. V. Bhosale, A Diketopyrrolopyrrole and Benzothiadiazole Based Small Molecule Electron Acceptor: Design, Synthesis, Characterization and Photovoltaic Properties, *RSC Adv*., 2014, **4**, 57635–57638.

21 M. J. Frisch, *et al.*, Gaussian 09, Revision D.01, Gaussian, Inc., Wallingford CT, 2016.